21, rue d'Artois, F-75008 PARIS
http : //www.cigre.org

CIGRE US National Committee
2013 Grid of the Future Symposium

Time Series Model of Photovoltaic Generation for Distribution Planning Analysis

Jorge Valenzuela
National Grid
United States

SUMMARY

Due to the often time consuming, complex and costly nature of electric systems modifications, analysis and planning of such systems normally requires a mid to long term planning approach. In this scenario, planners are required to make recommendations, for necessary changes or possible improvements, based on projections of the future condition of the system. Recently, the increasing introduction of renewable energy sources to distribution systems has raised questions about the impact that these new generating sources could have on the operating condition of the current infrastructure. Much of the analysis to date has been centered on acceptable limits of penetration of these installations and how they could affect the installed equipment and operation conditions. However, very little has been done to give guidance to distribution planners on how to represent these new energy sources during their mid to long term studies. The present work will introduce a time series model for photovoltaic (PV) generation, based on real data, designed to be used in distribution planning analysis. After validation, the model will be used to make an assessment of the changes in the conditions on the system under different levels of PV generation penetration and how this affects the decision making process of distribution planning.

KEYWORDS

Solar generation modeling, Hourly Solar Irradiation model, Distribution planning analysis, Time series decomposition, Seasonal decomposition.

Jorge.Valenzuela@nationalgrid.com

1. INTRODUCTION

As characterized by EISA [1] and summarized by EPRI in its 2011 report [2], Smart Grid refers to a modernization of the electricity delivery system so that it monitors, protects and automatically optimizes the operation of its interconnected elements. This effort includes, as one of its main components, the deployment and integration of distributed resources and generation, including renewable resources. The strategy followed to increase the penetration of these Energy Sources has come in the form of regulatory requirements derived from states' laws. For example, Section 11F and 11F1/2 of the Massachusetts's Division of Energy Resources established a Renewable Energy Portfolio and Alternative Energy Portfolio Standard to address this initiative. Such sections require that every retail supplier provides a minimum percentage of energy coming from Renewable or Alternative Energy Sources to the end customer.

Currently, the use of net metering and government incentives has resulted in an increase of applications for interconnection of distributed resources in distribution systems. For example, according to the most recent data presented by the Department of Energy Resources of the State of Massachusetts [3], the applications submitted to National Grid in the State of Massachusetts have been increasing at a rate of 40% a year (NY rate increase was up to 30%). Out of that percentage, almost 90% comes from a renewable energy sources. This increase on integration of renewable sources to National Grid's distribution system will continue to change its operational nature.

From a planning perspective, when conducting long-term system studies, distribution planners would normally make their estimations considering that local distributed generation sources (typically few in number and of known sizes) are fixed to either the nameplate or "OFF" as a way to be "conservative". These assumptions might work in scenarios that are focused on identifying system's normal or contingency "thermal" performance. However, they can lead to gross inaccuracies when in presence of an increasing number of variable generation units, like renewable ones.

This paper presents a procedure for modeling of power generation from a solar unit in a distribution system with the intention of using it to create distribution planning guidelines.

2. Characteristics of Solar Power Generation

Power Generation of a solar array is mainly dependant of the Sun's position in the sky. Such position is determined by the panel's geographical location and the time of the day. Figure 1 shows a graph of power generation from a 983 kW National Grid solar unit located in Worcester, Massachusetts [4].

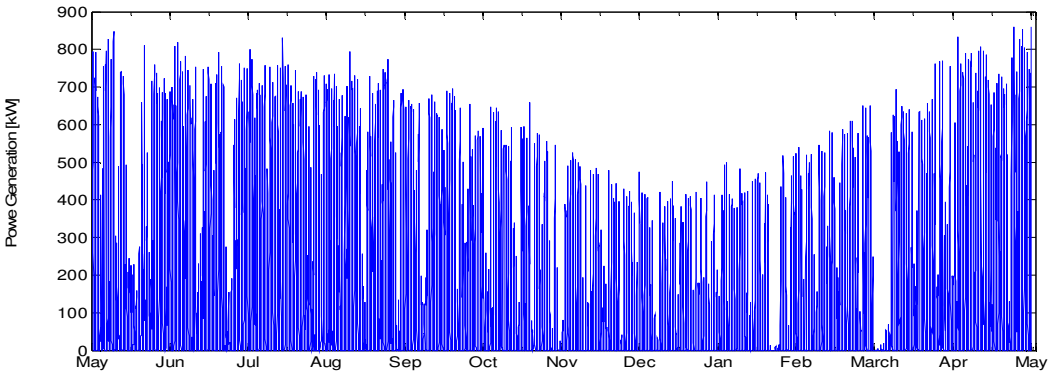

Figure 1 Power Generated by National Grid's 1 MW Solar installation in Worcester, MA

As can be clearly seen from the graph, the peak and low points of generation for the unit occur during the summer and winters solstice respectively. This is due to the position of the Sun related to the latitude and longitude (Northern Hemisphere) of the location where the generation unit is. As Figure 2 shows [5-6], power generation in the unit basically follows the elevation angle of the Sun through the year, peaking on Jun 21 and reaching its lowest point on Dec 21.

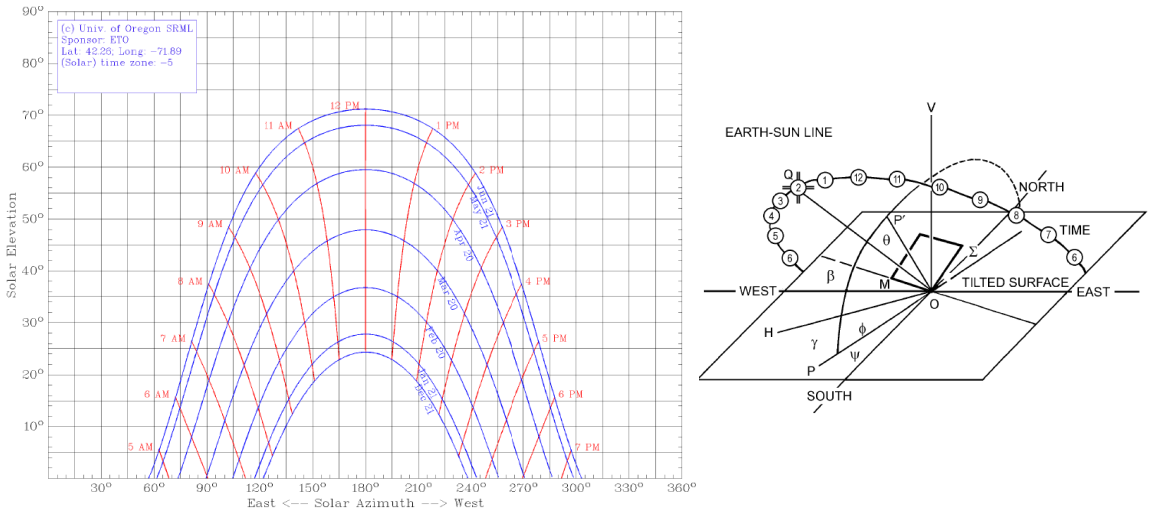

Figure 2 (a) Left: Sun's path during a calendar year in Worcester, MA [5]
(b) Right: Generic diagram of the Sun's movement above the horizon [6]

Therefore, a time model of solar generation requires the use of a solar irradiation model that includes the Sun's positioning component.
In basic terms, the total irradiation hitting any surface at any given time is given by:

$$I_T = I_D * \cos(\theta) + I_d + I_r \text{ with } I_D = A * e^{-B/\sin(\beta)} ; I_d = C * I_D * F_{SS} ; I_r = I_{tH} * \rho_g * F_{sg} \quad (1)$$

Where I_T: Total Solar irradiation [W/m^2]
θ: Incident angle
I_D: Direct normal irradiation [W/m^2]
I_d: Diffuse irradiation [W/m^2]
I_r: Reflected irradiation [W/m^2]
A: Apparent solar irradiation coefficient
B: Atmospheric extinction coefficient
β: Solar altitude angle
C: Ratio of diffuse radiation on a horizontal surface to the direct solar radiation
F_{SS}: Angle factor between surface and sky
ρ_g: Foreground reflectivity
F_{Sg}: Angle factor between surface and ground

In Equation 1, the irradiation variability through the year is introduced, for the most part, by time and seasonal changes on the incident and solar altitude angles. The relationships used to obtain these angles are presented in the set of Equations 2.

$$\begin{aligned} &\sin(\beta) = \cos(LAT) * \cos(\delta) * \cos(H) + \sin(LAT) * \sin(\delta) \\ &H = ((Time(\text{mins}) - 720)/4) * 15^\circ \quad ; \quad \delta = 23.45^\circ * \sin\left(360^\circ * (284 + N)/365\right) \\ &\cos(\theta) = \sin(\beta) * \cos(T) + \cos(\beta) * \sin(T) * \cos(\alpha_1 - \alpha_2) \\ &\alpha_1 = \cos^{-1}((\sin(\beta) * \sin(LAT) - \sin(\delta))/(\cos(\beta) * \cos(LAT))) * \text{sgn}(H) \end{aligned} \quad (2)$$

Where δ: Declination angle
H: Number of sun hours
LAT: Latitude angle
N: Day Number (1=January 1st)
T: Tilt of the solar panel
α_1: Solar azimuth angle
α_2: Azimuth angle of the solar panel

For comparison purposes, Equations 1 and 2 are used to obtain a solar irradiation yearly graph for the city of Worcester, Mass. Figure 3 shows an overall comparison between measured values and the calculated ones in per unit of their yearly maximum values. In the case of irradiation obtained by Equation 1, the procedure requires the elimination of all the values obtained when the solar altitude angle reaches negative values, that is, when the Sun's position is calculated to be below the horizon.

The seasonal behavior through the year of the calculated values follows the measured ones and, as Figure 4 shows, there's also a relatively close match between the daily measurements and the calculated values considering clear sky conditions.

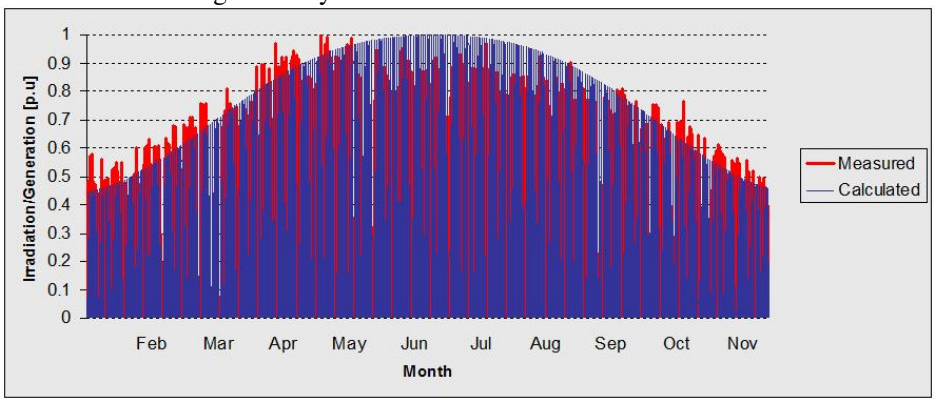

Figure 3 Calculated values of solar irradiation versus measured power generation through the year

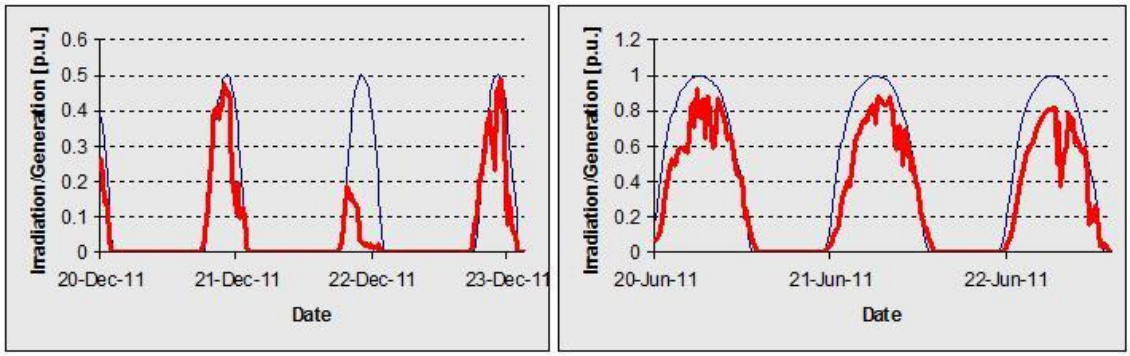

Figure 4 Detail of calculated irradiation versus measured power generation

Further adjustments will be introduced in the next section to compensate for errors and random behavior of irradiation.

3. Numerical characterization and error compensation

As it was noted in previous section, the theoretical model is valid under a clear sky scenario and suffers from some non-linear behavior which is difficult to represent in a set of equations that are easy to use. In addition, to really represent solar generation, it is necessary to add some level of compensation to the model to capture effects of energy conversion, temperature and/or clouds as noted by the discrepancies between the measured and calculated values in Figure 4. An analysis of the error, generated by the difference between the model and measurements, can be seen in Figure 5. After running a seasonal additive decomposition [7] of a year worth of data, considering a periodicity of 1 day, it can be seen that the trend component is the main source of discrepancy between the measured and the calculated values. Figure 5 also shows that the trend shows a behavior similar to a sine wave with a period equal to two years.

As the discrepancies are just present during the time while the Sun is above the horizon, the introduction of random behavior, such as clouds or even temperature changes, requires an expression that makes them active only when the Sun is visible.

In the notation already used, Sunrise (and Sunset) times through the year can be calculated using Equation (3).

$$SS = 720\,\text{min} \pm \cos^{-1}(-\tan(L) * \tan(\delta)) * 4\,\text{min/deg} \quad [\text{min}] \tag{3}$$

Using these calculated times it is possible to obtain a function that represents the period when the Sun is above the horizon. This function, expressed by Equation 4, can be used to remove all the negative portions of the calculated value of irradiation since they are not physically possible in real life. Therefore, the power generation model, considering scaling factors, errors and random behavior, can be modeled by the time series represented by Equation 5.

$$SV(t) = \sum_{N=1}^{365} u\left(t - \left(1440 * N - 720 - \cos^{-1}(-\tan(L) * \tan(\delta)) * 4\right)\right) + u\left(t - \left(1440 * N - 720 + \cos^{-1}(-\tan(L) * \tan(\delta)) * 4\right)\right) \quad \text{t in minutes} \tag{4}$$

$$P_g = P_{Nom} * \left(0.9 * I_T - 0.23 * \sin(2 * \pi * (t + 14400) / 1051200) * \text{rand}(t)\right) * SV(t) \tag{5}$$

Where $u(t)$: Step function
rand(t): Random variable normally distributed (0-1)
P_{Nom}: Nominal Power of the Unit (kW)
I_T: Total solar irradiation (p.u.)

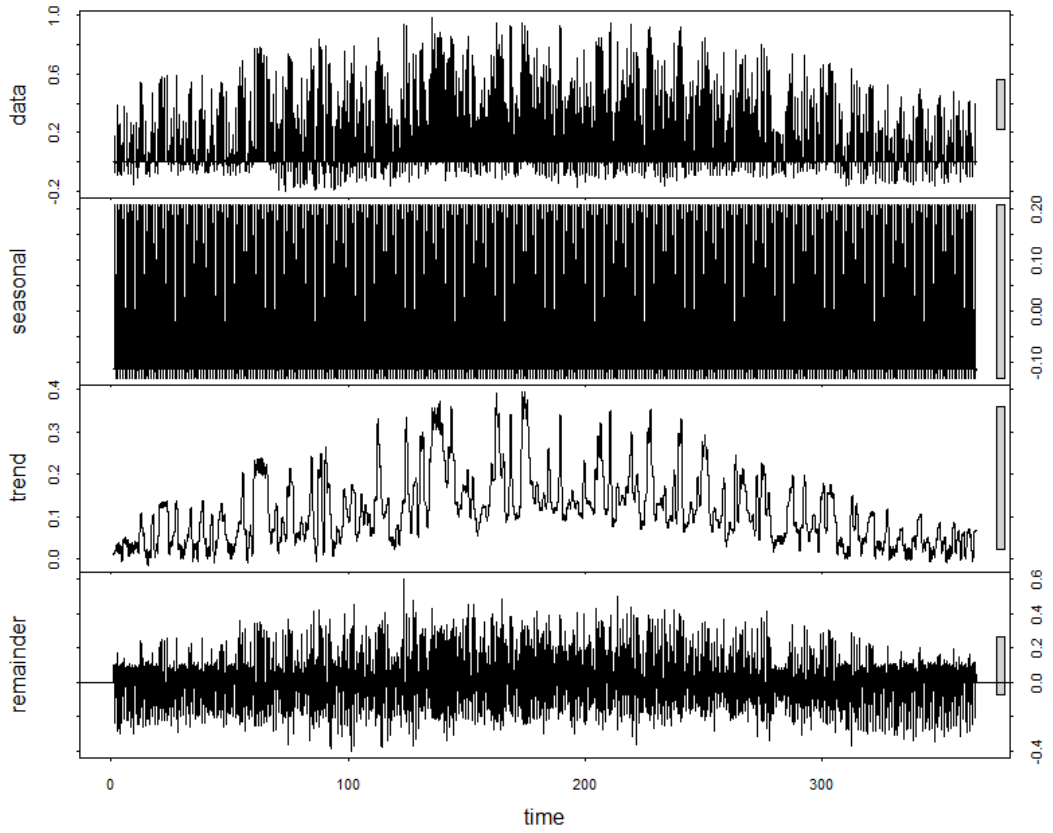

Figure 5 Additive seasonal decomposition of the error between calculated irradiation and measured power generation values

4. Use of the solar generation model for distribution planning analysis

In general terms, and due to the amount of work involved, distribution planning analysis is done considering a medium to long term timeframe. During the calculations, special importance is given to extreme conditions to obtain capacity limitations or abnormal conditions that the system could face. Summer peak conditions are generally considered as the upper operation boundary for the system, dominating the emphasis of the infrastructure development. Figure 6 shows a graph of the load

readings for a typical National Grid's 13.8kV distribution feeder of the city of Worcester, MA and the corresponding solar generation for that time. As the graph shows, most of the feeder's day peak levels for this time of the year and location are registered at about 4:00PM. At that time, the solar power generation is, under clear sky conditions, close to 50% of the nameplate of the generation unit. This is also true for the feeder's year peak, which is shown in the graph for July 21. It should be noted that the summer's load peak condition for the feeders in the area generally occurs in days with relatively clear sky conditions (as with the case shown in Figure 6), therefore the use of this type of calculated value for solar generation when doing the analysis is appropriate for the area under review.

This finding is significant and should be considered when setting up a review of capacity constraints in the area of analysis. Planners could use this as a parameter for setting up their solar generation levels during summer's peak capacity conditions in the Worcester area. Other locations may require different considerations depending on the typical weather conditions for the area during peak times (ex: areas where peak loading normally occurs under heavy haze, etc.). By obtaining a good estimate for solar generation during feeders' peak conditions planners will not only generate more accurate planning studies but will also be in a better position to make assessments on the effect, and potential limits, of high penetration of PV installations in the area.

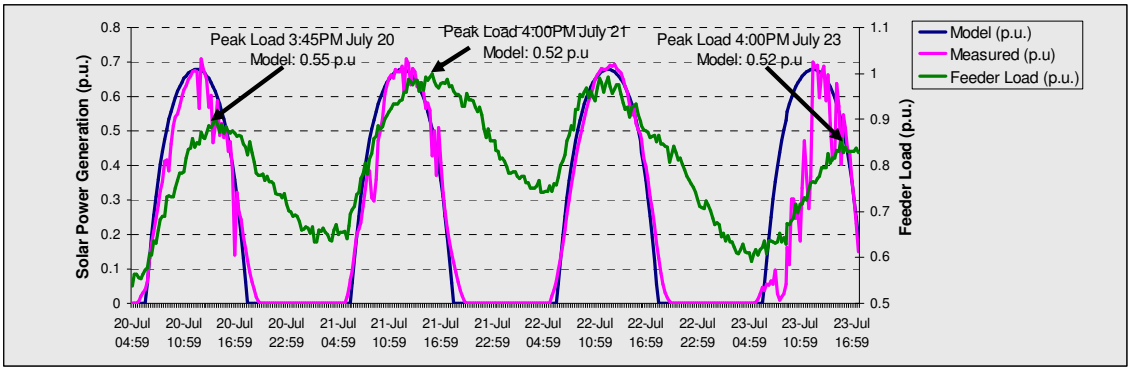

Figure 6 Solar power generation and feeder loading during summer peak conditions in the city of Worcester, MA

Another case of interest, from an operational point of view, is the review of light load conditions. During those periods, undesirable effects such as power backflows and overvoltage could occur due to the relative increase in importance of solar generation on the system. As it can be seen in Figure 7, the loading level in the particular feeder under study is at its lowest in the season when most of the solar generation is achieved.

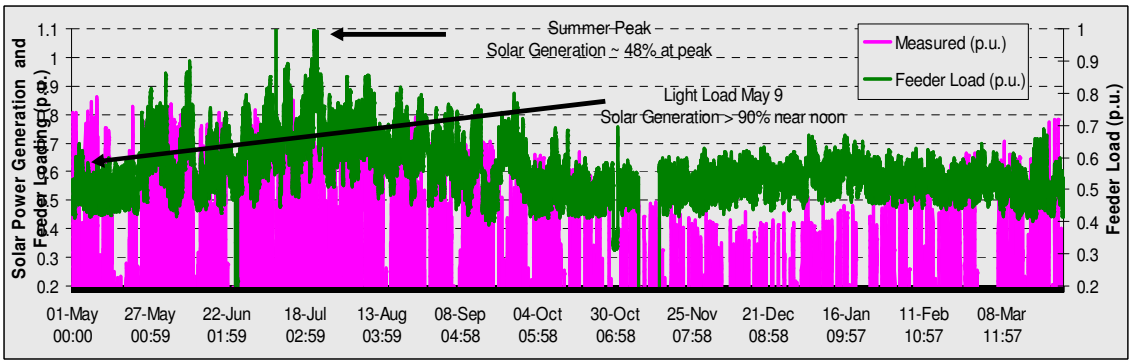

Figure 7 Solar power generation and feeder loading in Worcester, MA through the year

Figure 8 shows a comparison between the feeder load and the actual solar generation measurements. It can be seen that while the feeder loading reaches approximately 55% of its annual peak, solar generation can reach more than 80% of the nameplate of the unit near noon time. This magnitude of

solar generation can be easily obtained using the model with a clear sky condition as well, where the maximum generation is obtained for that time of the year.
This indicates that the feeder is more vulnerable to overvoltage issues and having sections with power backflow during that period of the year and time. Planners, when presented with this scenario, should prepare their controlled reactive support and local protection schemes accordingly to mitigate any degradation to the quality of service in areas where penetration of solar installations is expected to be high.

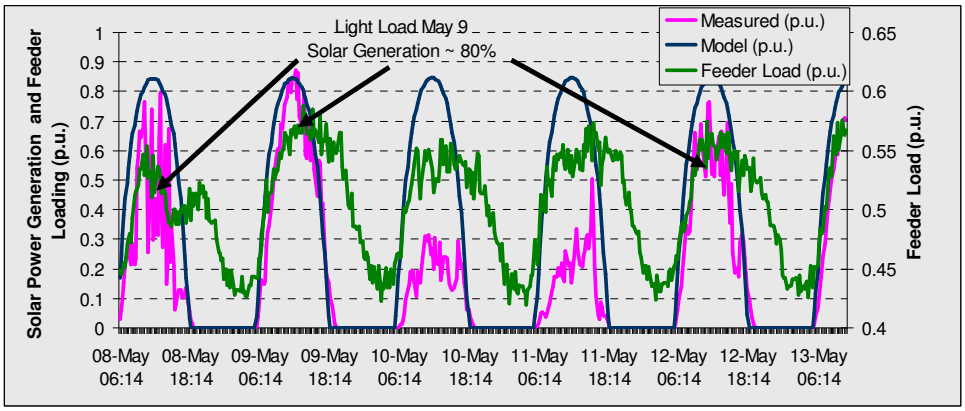

Figure 8 Solar power generation and feeder loading during light load conditions in Worcester, MA

5. Conclusions, comments and future work

National Grid is currently in the implementation phase of its Smart Grid Pilot in the city of Worcester, MA. This project will enable the collection of electrical quantities in diverse areas of its distribution system. Within those areas, several transformer monitors will be installed, mainly, to collect detailed information of the behavior of renewable energy sources. This collection of data will allow National Grid to verify the quality of its actual models and analysis procedures.
In preparation for the upcoming influx of data from the intelligent devices to be deployed in the field, and following its tradition of constant improvement of its analysis tools, the National Grid Advanced Engineering group is currently preparing models and guidelines that will help to advise the rest of the organization on ways to improve their analysis methodologies. The solar generation model presented in this paper falls into this category. By creating an easy way to obtain a time-based approximation of solar generation, planners will be better positioned to set up their simulations under different conditions, creating more efficient and precise results. Without having to rely on more sophisticated simulation packages, planners will be able to make a quick assessment on how much the appropriate solar generation level should be used for the system conditions they are trying to analyze.
The model is relatively easy to use and, as it can be seen in Figure 6 and 8, it represents with a good level of accuracy at the times when the solar generation will be present at a given location through the year and the expected solar generation values under clear sky conditions. It requires, however, some level of calibration, for which location's dependency is yet to be determined, to adjust to the specific measurements. As the solar generation data continues to become more readily available, especially by initiatives like National Grid's Smart Grid pilot, these models can be perfected and generalized for other sets of conditions and locations. It is clear that the trend component shown in Figure 5 has more information than it was really used for in the clear sky model. There is a more accurate and detailed analysis that has to be done to represent the random behavior of clouds, humidity and temperature. For example, it is expected that some periods of the year will have a series of cloudy days with a different level of correlation, that is, the probability of having a cloudy day after a cloudy day has occurred in November or December is probably higher than in July. There is also the need to analyze correlations between customer's behavior and solar generation. For example, Figure 6 shows the feeder's load curve having a different behavior during July 22. This can be explained by the amount of heat felt on July 21 and how that is going to modify the behavior of the customers who might decide to leave their air conditioners "ON" during the night or starting them early in the day to avoid

experiencing the same level of discomfort they felt the day before. Although this doesn't change the behavior of solar irradiation it does move the feeder's daily peak, changing the potential impact that solar generation could have on the system. Despite the fact that these specific analyses weren't carried out during the course of this particular work, the creation of a "Sun Visibility" function (Equation 4) is going to facilitate the incorporation of such random behavior characteristics into the clear sky model, making it more accurate and descriptive of the phenomenon.

BIBLIOGRAPHY

[1] US Congress, "Energy Independence and Security Act 2007", (Available from http://www.gpo.gov/fdsys/pkg/PLAW-110publ140/pdf/PLAW-110publ140.pdf, Dec. 2007, [Accessed June 2013]).

[2] EPRI, "Estimating the Costs and Benefits of the Smart Grid", (Available from http://my.epri.com/portal/server.pt?Abstract_id=000000000001022519, Mar 2011, [Accessed June 2013]).

[3] Kema Inc., "Massachusetts Distributed Generation Interconnection Report, Final Report", (Available from http://www.mass.gov/eea/docs/doer/renewables/dg-inter.pdf, Jul 2011. [Accessed June 2013]).

[4] National Grid – Delivery Services, "Sutton/Northbridge Solar Power Project", (http://www.nationalgridus.com/masselectric/solar/sutton.asp, 2013, [Accessed June 2013]).

[5] UO SRML: Sun path chart program [online] (Available from: http://solardat.uoregon.edu/SunChartProgram.html, 2007, [Accessed June 2013]).

[6] American Society of Heating, Refrigerating and Air-Conditioning Engineers, "2011 ASHRAE Handbook - Heating, Ventilating, and Air-Conditioning Applications (I-P Edition)", (ISBN: 978-1-936504-06-0, Apr 2012).

[7] R. B. Cleveland, W. S. Cleveland, J.E. McRae, and I. Terpenning, "STL: A Seasonal-Trend Decomposition Procedure Based on Loess", (Journal of Official Statistics, 6, 3–73, 1990).